

## Hot Paper

Chromium Complexes with Benzanellated N-Heterocyclic Phosphenium Ligands—Synthesis, Reactivity and Application in Catalytic CO<sub>2</sub> ReductionNicholas Birchall,<sup>[a]</sup> Fridolin Hennhöfer,<sup>[a]</sup> Martin Nieger,<sup>[b]</sup> and Dietrich Gudat\*<sup>[a]</sup>

A chromium complex carrying two benzanellated N-heterocyclic phosphenium (bzNHP) ligands was prepared by a salt metathesis approach. Spectroscopic studies suggest that the anellation enhances the  $\pi$ -acceptor ability of the NHP-units, which is confirmed by the facile electrochemical reduction of the complex to a spectroscopically characterized radical anion. Co-photolysis with H<sub>2</sub> allowed extensive conversion into a  $\sigma$ -H<sub>2</sub>-complex, which shows a diverse reactivity towards donors and isomerizes under H–H bond fission and shift of a hydride to a P-ligand. The product carrying phosphenium, phosphine and hydride ligands was also synthesized independently and reacts reversibly with CO and MeCN to yield bis-phosphine complexes

under concomitant Cr-to-P-shift of a hydride. In contrast, CO<sub>2</sub> was not only bound but reduced to give an isolable formate complex, which reacted with ammonia borane under partial recovery of the metal hydride and production of formate. Further elaboration of the reactions of the chromium complexes with CO<sub>2</sub> and NH<sub>3</sub>BH<sub>3</sub> allowed to demonstrate the feasibility of a Cr-catalyzed transfer hydrogenation of CO<sub>2</sub> to methanol. The various complexes described were characterized spectroscopically and in several cases by XRD studies. Further insights in reactivity patterns were provided through (spectro)electrochemical studies and DFT calculations.

## Introduction

Cooperative reactivity of a metal and its ligand sphere has lately emerged as a concept to circumvent the preference of many complexes of first-row (3d) transition metals for reactions involving one-electron redox steps and enable these species to undergo oxidative additions or reductive eliminations that are commonly viewed as two-electron redox processes.<sup>[1]</sup> The implementation of this metal-ligand cooperativity (MLC) is often achieved by the use of redox non-innocence to create ligands that can either actively participate in substrate binding and activation, or are non-reactive but act as an electron reservoir to stimulate two-electron reactivity.<sup>[1,2]</sup> Oxidative addition and reductive elimination being pivotal steps in many organometallic transformations, the ability to undergo such reactions also facilitates the application of first-row transition metal complexes in homogeneous catalysis<sup>[1]</sup> and makes them possible alternatives to the traditional noble (4d or 5d) metal-based catalysts. A growing interest in such developments is

reflected by the continuing elaboration of first-row transition metal catalysts for reactions like alkene and alkyne hydrogenation that are typically carried out on catalysts based on noble metals.<sup>[2]</sup>

In this context, we have recently reported on the use of chromium complexes **1 a,b** carrying two N-heterocyclic phosphenium (NHP) ligands as pre-catalysts for the hydrogenation of various alkenes and alkynes (Scheme 1).<sup>[3,4]</sup>

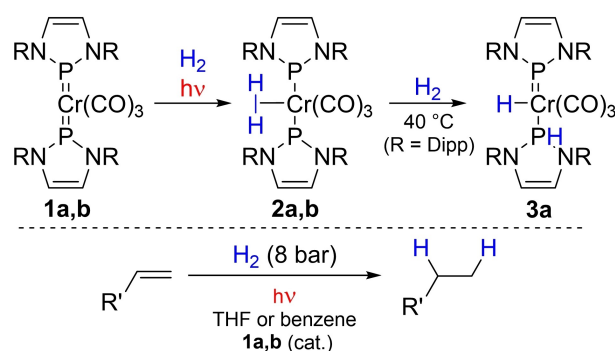
The initiation of the catalysis by the photochemical generation of H<sub>2</sub>-complexes **2 a,b** relies vitally on the excitation of a MLCT transition to generate a vacant coordination site in the electronically saturated (18 VE) precursors **1 a,b**. The NHP units act in this process as electron reservoirs<sup>[1]</sup> that facilitate two-electron reactivity. Complexes **2 a,b** may then react with alkenes or alkynes as stoichiometric H<sub>2</sub>-transfer reagents that require regeneration after each turnover.<sup>[4]</sup> Moreover, **2 a** was reported to isomerize in the absence of an organic substrate under fission of the H–H bond and transfer of one hydrogen

[a] N. Birchall, F. Hennhöfer, D. Gudat  
Institut für Anorganische Chemie, University of Stuttgart, Pfaffenwaldring  
55, 70550 Stuttgart, Germany  
E-mail: gudat@iac.uni-stuttgart.de  
Homepage: <https://www.iac.uni-stuttgart.de/forschung/akgudat/>

[b] M. Nieger  
Department of Chemistry, University of Helsinki, P.O. Box 55, 00014 Helsinki,  
Finland

Supporting information for this article is available on the WWW under  
<https://doi.org/10.1002/chem.202401714>

© 2024 The Authors. Chemistry - A European Journal published by Wiley-VCH  
GmbH. This is an open access article under the terms of the Creative  
Commons Attribution License, which permits use, distribution and re-  
production in any medium, provided the original work is properly cited.



Scheme 1. Reported<sup>[3,4]</sup> photo-induced binding of H<sub>2</sub> to bis-NHP complexes **1 a,b** and their use in alkene hydrogenation (R=Dipp (**1 a–3 a**), Mes (**1 b, 2 b**)).

atom to a NHP ligand to give **3a** representing the product of hydrogenolysis in which the H<sub>2</sub> molecule has been added across a metal-phosphorus double bond of **1a**.<sup>[3]</sup>

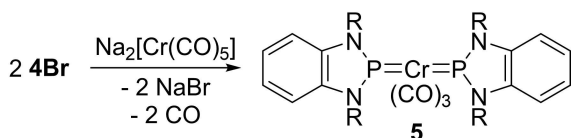
Having noticed that the NHP moieties exert a visible influence on the behavior of **2a,b** in hydrogenation processes, we wanted to understand this effect in more detail. Apart from tuning the electronic and steric properties of the NHP ligands by varying N-substituents, it should also be feasible to adjust the acceptor character by modifying the  $\pi$ -electron system in the heterocycle. Benzenellated N-heterocyclic phosphonium (bzNHP) ions<sup>[5–8]</sup> like **4<sup>+</sup>** (Scheme 2) have delocalized  $10\pi$ -systems extending over both rings and comparable aromatic stabilization energies as their monocyclic congeners,<sup>[9,10]</sup> and are thus expected to show superior  $\pi$ -acceptor character. We report here on the synthesis, characterization, and selected chemical reactions of analogues of **1a,b** and **3a** with bzNHP-ligands. The results of these studies illustrate how benzenellation affects the electronic properties of the NHP ligands and the chemical behavior of the complexes.

## Results and Discussion

The synthesis of complex **5** with two bzNHP ligands (Scheme 3) was achieved like that of **1a**<sup>[11]</sup> via metathesis of Na<sub>2</sub>[Cr(CO)<sub>5</sub>] with bromo-benzodiazaphospholene **4Br**, which had been prepared from the appropriate phenylene diamine by



**Scheme 2.** Molecular structures of a bzNHP ion (**4<sup>+</sup>**) and a benzannellated N-heterocyclic phosphine **4X** (X = any substituent, R = Dipp).



**Scheme 3.** Synthesis of complex **5** (R = 2,6-*i*Pr<sub>2</sub>C<sub>6</sub>H<sub>2</sub> ≡ Dipp).

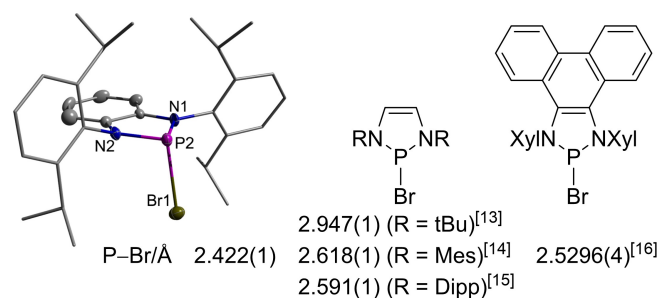


**Figure 1.** Molecular structure of **4Br** in the crystal (left; hydrogen atoms were omitted for clarity and thermal ellipsoids were drawn at the 50% probability level) and molecular formulae of previously reported reference compounds (data from refs.<sup>[13–16]</sup>). Given figures denote the P–Br distances (in Å).

dilithiation<sup>[12]</sup> and subsequent salt metathesis with PBr<sub>3</sub>. The products **4Br** and **5** were isolated in crystalline form and identified by analytical and spectroscopic data and single-crystal X-ray diffraction (XRD) studies.

The molecular structure of **4Br** in the crystal features a P–Br distance that is clearly shorter than in other known bromo-diazaphospholene derivatives (Figure 1). Considering that P-halogeno-diazaphospholenes have been described as Lewis-acid/base complexes with dative P–X bonds whose distances reflect the different degree of interaction between halide anion and diazaphospholenium cation fragments, the short P–Br bond in **4Br** can be seen as a first hint that benzenellation increases the Lewis-acidity (and thus the electron accepting character) of the NHP cation fragment.

The molecules of **5** (in a crystalline solvate with two disordered molecules of pentane per formula unit, Figure 2) contain penta-coordinate metal centers and bzNHP ligands showing the short phosphorus-metal distance and planar coordination around phosphorus that are typical for a 'phospho-Fischer carbene' bonding mode with formal P–Cr double bonds.<sup>[17]</sup>

The molecular shape is qualitatively similar as in the known analogues **1b**<sup>[4]</sup> and **1a**<sup>Si[11]</sup> with monocyclic NHP ligands, but the P1–Cr1–P2 angle is clearly larger than in the reference compounds, and the metal coordination environment must hence be classified as intermediate between trigonal bipyramidal and square pyramidal (geometry index  $\tau_5$ <sup>[18]</sup> = 0.56). The P–Cr distances in **5** are indistinguishable and likewise slightly larger than in **1b** and **1a**<sup>Si</sup> (see Figure 2). The fused ring system adopts no envelope conformation as in **4Br**, but a planar alignment that is in accord with the presence of a delocalized  $\pi$ -electron system.<sup>[9,10]</sup> Comparing metric parameters with those of the cation of the crystalline phosphonium salt **4**[AlCl<sub>3</sub>Br] (Figure S23 and Table S5) reveals a lengthening of the endocyclic P–N and N–C distances, which indicates that the perturbation of the aromatic  $10\pi$ -system of the free cation by back-donation from the metal center results in the expected reduction of  $\pi$ -bond orders in the NHP unit.

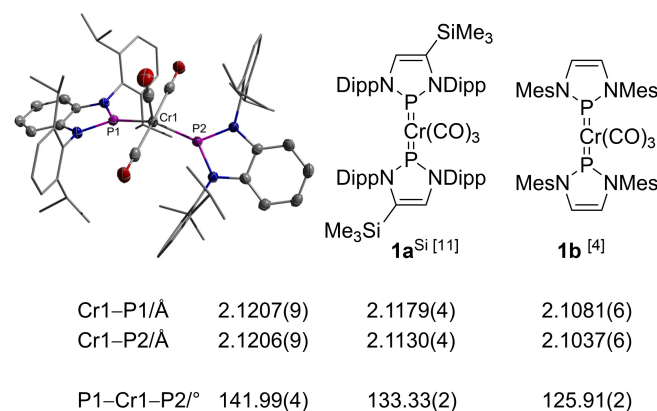


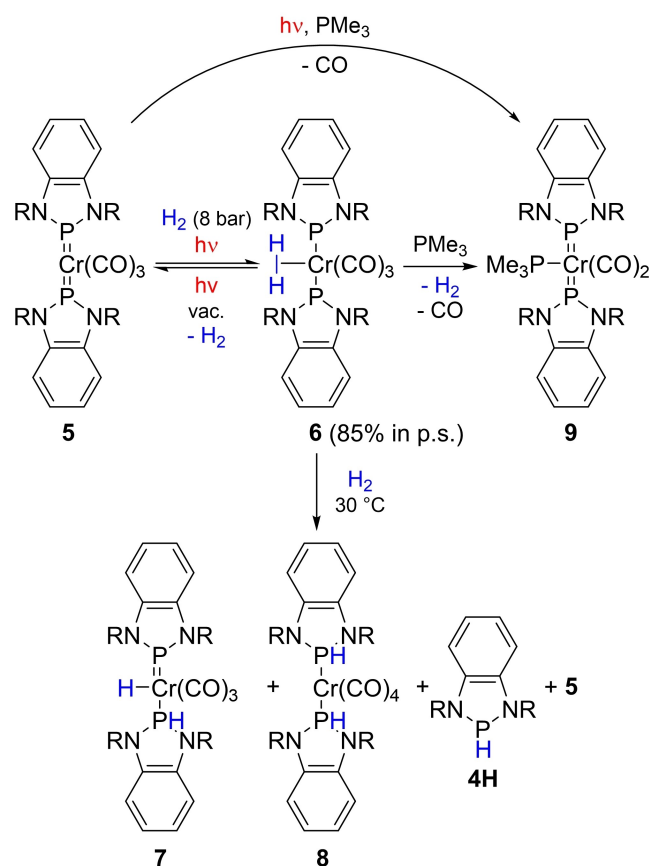
**Figure 2.** Molecular structure of **5** in the crystal (left; hydrogen atoms were omitted for clarity and thermal ellipsoids were drawn at the 50% probability level) and molecular formulae of previously reported analogues (data from refs.<sup>[4,11]</sup>). Given figures denote Cr–P distances (in Å) and P–Cr–P angles (in °).

While the  $^{31}\text{P}$  chemical shifts of **5** ( $\delta^{31}\text{P}$  238.8) and **1a** ( $\delta^{31}\text{P}$  238.0)<sup>[11]</sup> are essentially identical, the observed blue shift for the highest  $\nu_{\text{CO}}$  mode in the IR spectrum of **5** ( $1979\text{ cm}^{-1}$  vs.  $1964\text{ cm}^{-1}$  for **1a**)<sup>[3]</sup> further supports our initial conjecture that the benzenellation increases the net  $\pi$ -acceptor character of the NHP ligands. The coincidence of this trend with a lengthening of the P–Cr bonds appears at first glance counterintuitive, but can be rationalized by assuming that the consolidation of Cr→P  $\pi$ -bonding is offset by a weaker P→Cr  $\sigma$ -donor contribution.

A final confirmation of the trend in the  $\pi$ -acceptor properties of **1a** and **5** is derived from a comparison of their optical spectra and electrochemical behavior. The energetically lower of two distinctive absorption bands observable in the UV-VIS spectra of both species (Figure S39) arises according to a TDDFT study from a MLCT transition associated with electron excitation from a metal-dominated KS-HOMO into a KS-LUMO composed mainly of  $\pi^*$ -orbitals on both bzNHP ligands (Figure S62). The red-shift of this band in case of **5** ( $\Delta\lambda_{\text{max}} = 9\text{ nm}$ ) implies then that the lowest  $\pi^*$ -orbital is energetically more easily accessible and the bzNHP thus indeed a superior  $\pi$ -acceptor.

In accord with the conclusion derived from the optical spectra, cyclic voltammetry (CV) confirmed that **5** is more easily reducible than **1a**, undergoing partially reversible reduction at a half-wave potential of  $-2.69\text{ V}$ , while **1a** turned out to be inert within the accessible solvent window (Figure S1a). Characterization of the resulting radical anion [**5** $^{\cdot-}$ ] by EPR spectroscopy and UV-VIS-spectro-electrochemistry (SEC) revealed an EPR-signal with a large hyperfine splitting to two equivalent  $^{31}\text{P}$  nuclei ( $a = 90.3\text{ G}$ , Figure S1f) and the absence of a long-wave LLCT transition expected for a radical anion with localized (on a single NHP unit) spin density (Figure S1c). On top, IR-SEC (Figure S1b) exposed strong red-shifts for the  $\nu_{\text{CO}}$  modes of [**5** $^{\cdot-}$ ] compared to those of **5** indicating enhanced back donation from the Cr(NHP)<sub>2</sub>-moiety onto the CO ligands. All data together suggest that the reduction of **5** is mainly ligand-centered and the excess electron density is evenly distributed over both NHP units. This is also in accord with the results of DFT calculations predicting the localization of  $>80\%$  of the spin-density in [**5** $^{\cdot-}$ ] on the bzNHP ligands (Figure S63). The CV and SEC studies confirmed as well that prolonged electrolysis at constant potential produces follow-up products formed as the result of a second (irreversible) reduction process and possibly low thermal or chemical stability of [**5** $^{\cdot-}$ ].

To explore the behavior of **5** towards hydrogen, we studied its photolysis using the same conditions as for the generation of **2a** from **1a** (solution in THF- $d_8$  under 8 bar  $\text{H}_2$ , irradiation with a Xe arc lamp<sup>[3]</sup>). An NMR spectroscopic assay revealed that the reaction took a similar course, proceeding to a photostationary state characterized by the presence of a mixture of **5** and a  $\text{H}_2$ -complex **6** (Scheme 4). The identification of this species grounds on the discovery that its  $^{31}\text{P}$  NMR signal ( $\delta^{31}\text{P}$  234.2) gives rise to a  $^1\text{H},^{31}\text{P}$  HMQC correlation with a broad  $^1\text{H}$  NMR signal whose relative integral, negative chemical shift ( $\delta^1\text{H} -8.39$ ) and short  $T_1$  relaxation time ( $T_{1,\text{min}} 15.8\text{ ms}$  at  $-35^\circ\text{C}$ ) are archetypal for a metal bound  $\eta^2\text{-H}_2$ -ligand,<sup>[19–22]</sup> and is reinforced by the similarity of the observed data with those reported for **2a**<sup>[3]</sup> and **2b**<sup>[4]</sup>, respectively. Even if **6** could be enriched to up to



**Scheme 4.** Photolytic generation and thermal decay of  $\sigma\text{-H}_2$ -complex **6** (p.s. = photostationary state).

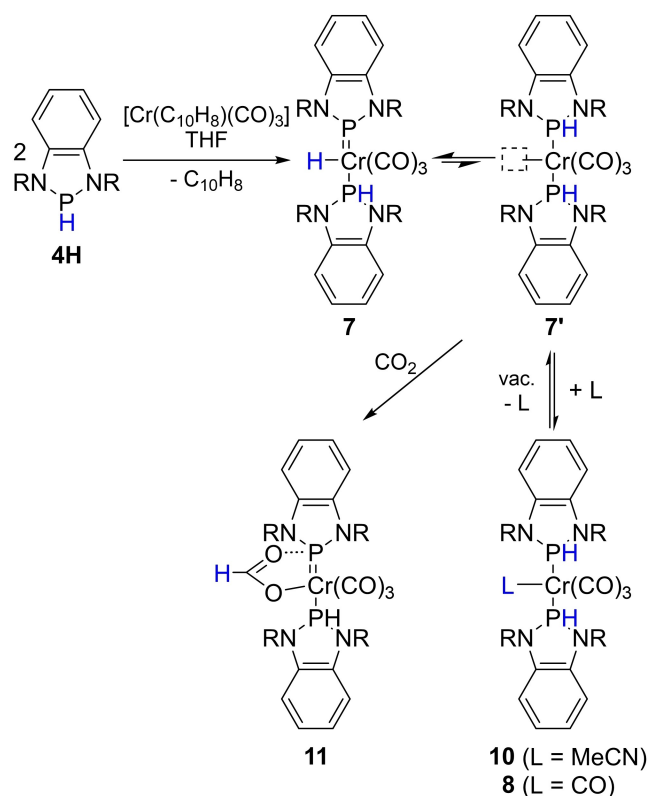
85% and was thus present in much higher concentration than **2a,b**, its isolation remained unfeasible, as in the case of its congeners.

Like **2a**,<sup>[3]</sup>  $\text{H}_2$ -complex **6** was observed to isomerize in the presence of excess  $\text{H}_2$  to yield a metal hydride complex **7** embodying the product of addition of  $\text{H}_2$  across a Cr–P double bond. NMR spectroscopy revealed that the reaction advanced slowly at mild conditions ( $30^\circ\text{C}$ ) to consume approx. half of the  $\text{H}_2$ -complex within 125 hrs. Unlike as with **2a**, this process was unselective, producing beside **7** also bis-NHP complex **5**, bis-phosphine tetracarbonyl complex **8** and free phosphine **4H** as further P-containing species (Scheme 4). The assignment of the new products was confirmed by independent synthesis (*vide infra* and Supporting Information). While thermally induced loss of  $\text{H}_2$  had already been noticed in case of **2b**,<sup>[4]</sup> the formation of **4H** and **8** implies the existence of a further decay pathway for **6** which involves the loss of phosphine and CO ligands and must also give rise to phosphorus-free by-products that could not be detected or specified. The competition of this fragmentation with the other reaction channels implies that **6/7** are thermally less stable than their congeners **2a/3a**, possibly because phosphine **4H** is a weaker  $\sigma$ -donor than the monocyclic secondary diazaphospholene contained in **2a** and is more easily cleaved.

Further studies of the behavior of **6** revealed that a controlled release of H<sub>2</sub> under near quantitative regeneration of bis-NHP complex **5** could be initiated by irradiation of a solution kept under autogenous pressure of the solvent (Scheme 4). To check whether the H<sub>2</sub>-ligand can not only be cleaved but also be substituted, we next studied the reactions of **6** with PMe<sub>3</sub>. The observation of the signals of a new AX<sub>2</sub>-spin system in the <sup>31</sup>P{<sup>1</sup>H} NMR spectrum of the reaction mixture confirmed that incorporation of the phosphine had indeed taken place. The same product formed also during irradiation of **5** in the presence of excess PMe<sub>3</sub> and was identified after isolation as dicarbonyl complex **9** (Scheme 4). A single-crystal XRD study (Figure S23) revealed a similar molecular structure as for **5**, except that the equatorial CO ligand had been formally swapped for PMe<sub>3</sub>. We presume that the phosphine reacts with **6** under initial replacement of H<sub>2</sub> to yield a transient tricarbonyl complex, which then relaxes via cleavage of CO. Interestingly, the reaction of **6** with CO took a different course, proceeding selectively under Cr-to-P shift of both hydrides to give **8** (see Supporting Information). The different behavior of CO and PMe<sub>3</sub> reflects presumably the different donor/acceptor properties of both ligands.

An attempt to utilize the conversion of **5** into **6** to drive the hydrogenation of styrene revealed that a catalytic transformation (according to Scheme 1) was in principle achievable. However, as full conversion of the substrate required much higher catalyst loading and longer irradiation time than the reactions with **1 a, b**<sup>[3,4]</sup> (see Supporting Information for details), these studies were not pursued further. While the low catalytic efficiency seems surprising if one considers that the driving force for the loss of H<sub>2</sub> is according to DFT calculations higher for **6** than for **2 a** (calculated standard Gibbs free energies ΔG<sup>0</sup> for this process are −29.6 kcal mol<sup>−1</sup> for **6** vs. −26.4 kcal mol<sup>−1</sup> for **2 a**) and **6** may thus be regarded to have higher potential energy, it is in accord with our earlier conclusion<sup>[4]</sup> that the hydrogenation appears to be favored when the electron donating character of the NHP units increases and their steric bulk decreases.<sup>[23]</sup>

The rational synthesis of **7**, which must be considered a key intermediate in the thermal decay of **6**, was achieved as published earlier<sup>[3]</sup> by treating [Cr(CO)<sub>3</sub>(naphthalene)] with two equivalents of phosphine **4H** (Scheme 5). The product was isolated in moderate yield after precipitation from Et<sub>2</sub>O and identified by spectroscopic data. A single-crystal XRD study suffered from severe disorder problems, but sufficed to confirm a molecular structure with one bzNHP and one secondary phosphine ligand (Figure S23). The spectroscopic data of **7** bear generally great similarity to those of **3 a**<sup>[3]</sup> featuring non-anellated NHP ligands, with two notable deviations: (i) the blue-shift of the νCO bands in the IR spectrum by some 10–20 cm<sup>−1</sup> with respect to **3 a** again pinpoints the higher net π-acceptor character of the benzenellated compared to monocyclic phosphenium and phosphine ligands, and (ii) the <sup>1</sup>H and <sup>31</sup>P NMR signals display strongly temperature dependent line shapes (see Figure S45) indicating accelerated scrambling of P- and Cr-bound hydrogen atoms. This conjecture is corroborated by DFT studies, which also confirm our earlier hypothesis<sup>[3]</sup> that



Scheme 5. Synthesis and reactivity of **7** (R=Dipp, C<sub>10</sub>H<sub>8</sub>=naphthalene)

the scrambling is achieved through a sequence of [1,2]-hydrogen shifts that establish a dynamic equilibrium between metal hydride (**3 a**, **7**) and bis-phosphine isomers (**3 a'**, **7'**, Figure 3). The calculations imply that the switch from monocyclic NHP to bzNHP units lowers not only the activation barrier for proton migration, but also stabilizes the bis-phosphine isomer.

In accord with computational predictions that benzenellation also favors attachment of an additional donor (Table S7), **7** reacted readily with ligands like CO and MeCN to give bis-phosphine complexes **8** and **10**, respectively (Scheme 5). Both

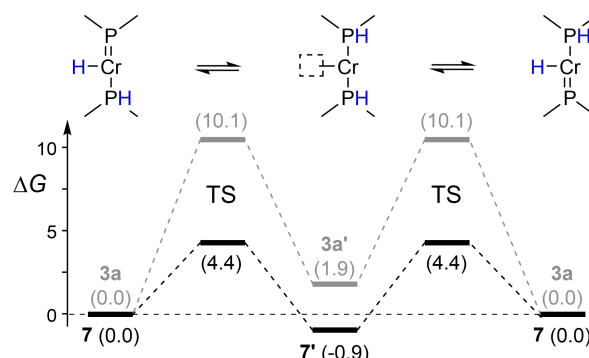
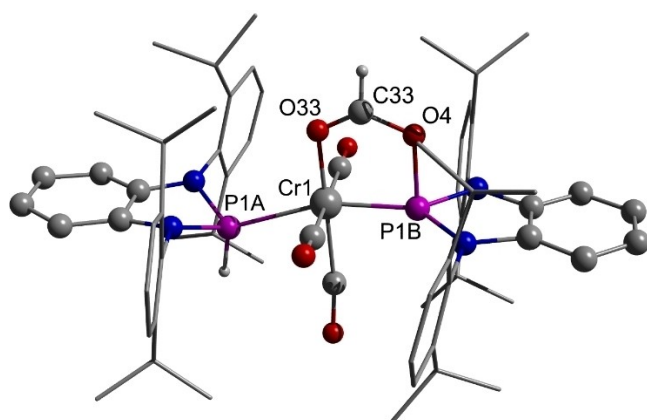


Figure 3. Schematic representation of the proposed mechanism for the scrambling of P- and Cr-bound H-atoms in complexes with simple (**3 a**/**3 a'**, grey) and benzenellated (**7**/**7'**, black) NHP moieties. Figures in parentheses denote relative Gibbs free energies ΔG<sup>0</sup> (in kcal mol<sup>−1</sup>) at the stationary states (calculations at the RI-ωB97X-D/def2-TZVP//RI-ωB97X-D/def2-SVP level of theory, see Supporting Information for further details).

products were isolated in crystalline form and identified by spectroscopic data and single-crystal XRD studies (see Figure S23). The higher Lewis-acidity of **7** compared to **3a** is reflected in the fact that quantitative conversion into **10** is already observed with the addition of a small amount of MeCN (1% solution) and the pure product does not visibly dissociate in solution,<sup>[24]</sup> whereas the MeCN-adduct of **3a** was even in the presence of high MeCN concentrations (> 14%) only detectable in equilibrium with **3a**.<sup>[3]</sup> That the formation of **8**, **10** is nonetheless reversible is illustrated by their partial reversion to **7** under vacuum. The different extent of this reaction (conversion of 78% after 30 min for **10** vs. 12% after 28 hrs for **8**) implies that MeCN is less tightly bound than CO as expected. Reversible formation of donor adducts is further presumed the key to explaining the reduced thermal stability of **7** in THF (see Supporting Information).

As a further example for the reaction of **7** with a weak donor, we studied its interaction with CO<sub>2</sub>. This case was considered attractive because O-coordination of CO<sub>2</sub> to the metal center of the coordinatively unsaturated isomer **7'** should activate the carbon atom for nucleophilic attack by an adjacent hydric PH-moiety and thus enable a similar hydrophosphination of CO<sub>2</sub> as in the reaction with a free secondary diazaphosfolene reported by the group of Kinjo.<sup>[25,26]</sup>

As anticipated, admission of CO<sub>2</sub> to a solution of **7** gave rise to a single product that was isolated by crystallization and identified by NMR spectroscopy and a single-crystal XRD study as the complex **11** (Scheme 5). The crystal structure suffered from a disorder of the whole complex molecule about a crystallographic center of symmetry which severely affects the interpretation of the data. Although we have finally arrived at a successful refinement that is suitable to confirm the molecular structure (see Supporting Information for details), a detailed analysis is still not possible and we will therefore refrain from discussing the metric parameters. The most prominent features of **11** are the presence of two inequivalent NHP units and a formate ligand which interacts in a  $\mu_2$ -bridging mode with the octahedrally coordinated chromium center and one of the phosphorus atoms (Figure 4). One phosphorus atom can be



**Figure 4.** Ball-and-stick representation of the molecular structure of **11** in the crystal. Hydrogen atoms except those bound to C33 and P1 A were omitted for clarity.

identified as part of a coordinated secondary phosphine and displays the expected tetrahedral coordination environment. The other phosphorus atom features a much shorter P–Cr bond and two P–N bonds in a nearly planar arrangement, and an additional secondary interaction to a formate oxygen atom that is roughly perpendicular to this plane. Hence, we describe the NHP moiety in this case as a ‘phospha-Fischer carbene’ ligand<sup>[17]</sup> engaged in an additional P $\cdots$ O dative interaction.

The structural assignment derived from the XRD study is backed by spectroscopic data. The <sup>31</sup>P NMR spectrum displays an AX pattern ( $\delta^{31}\text{P}$  157, 207; <sup>2</sup>J<sub>PP</sub> = 55 Hz) with deviating chemical shifts that are in accord with the presence of phosphonium and phosphine ligands, and the <sup>1</sup>H NMR spectrum contains a diagnostically revealing signal attributable to the P-bound hydrogen ( $\delta^1\text{H}$  8.67, <sup>1</sup>J<sub>PH</sub> = 303 Hz). The assignment of the <sup>1</sup>H NMR signal of the formate ligand ( $\delta^1\text{H}$  7.53) is confirmed by the observation of a highly specific<sup>[27,28]</sup> <sup>1</sup>H,<sup>13</sup>C HSQC correlation to the adjacent carbon atom ( $\delta^{13}\text{C}$  167).

Technically, the formate ligand of **11** may not only be formed through a cooperative process starting from **7'** as proposed above, but also by the direct transfer of the metal-bound hydride of the phosphonium isomer **7**. A computational model study on the reactions of **3a** and **7** with CO<sub>2</sub> suggests that both pathways are in principle feasible (Figure 5). Interestingly, the ‘outer sphere’ variant involving initial binding of CO<sub>2</sub> in a loose van-der-Waals complex and subsequent transfer of the metal-bound hydride (route A) was predicted to have the lower barrier for **3a** with monocyclic NHP units, while the ‘inner sphere’ pathway via formation of a  $\kappa^1\text{-O-CO}_2$ -complex and ensuing hydride transfer from a phosphine ligand (route B) was identified as kinetically slightly favored in case of **7**. Detailed analysis reveals that although this trend coincides with the lower  $\Delta G^\circ$  of the bis-phosphine isomer **7'** relative to **7** and a slight stabilization of the  $\kappa^1\text{-O-CO}_2$ -complex over the van-der-Waals complex, the main influence seems to come from the destabilization of the route A transition state, which in turn correlates with an increased separation between CO<sub>2</sub> and the reactive Cr–H functionality in the van-der-Waals complex. We posit that this effect reflects a reduced conformational flexibility of the bzNHP complex and is thus mainly of steric and not electronic origin.

Being aware that a free diazaphosfolene had not only been applied as a stoichiometric reagent but also as a catalyst in the reduction of CO<sub>2</sub>,<sup>[25,26]</sup> we envisaged that a catalytic use of **7** might likewise be in reach. Searching first for a route to recover the active reagent **7/7'**, we found that formate complex **11** is inert towards alkaline metal hydrides, silanes, and H<sub>2</sub>, but reacts with ammonia borane (AB). Even though this transformation is slow and unselective, it proved that partial recycling of **7** (42% with respect to the complex used, see supporting information for details) is indeed feasible and prompted us to investigate the use of **7** or **11** as catalyst in the transfer hydrogenation of CO<sub>2</sub> with AB. While this reaction is commonly mediated by stoichiometric quantities of external bases,<sup>[29–31]</sup> frustrated Lewis pairs,<sup>[32,33]</sup> or Ge(II) and Sn(II) hydrides,<sup>[34–36]</sup> respectively, Choudhury et al. reported recently on a first catalytic transfer hydrogenation of CO<sub>2</sub> to ammonium

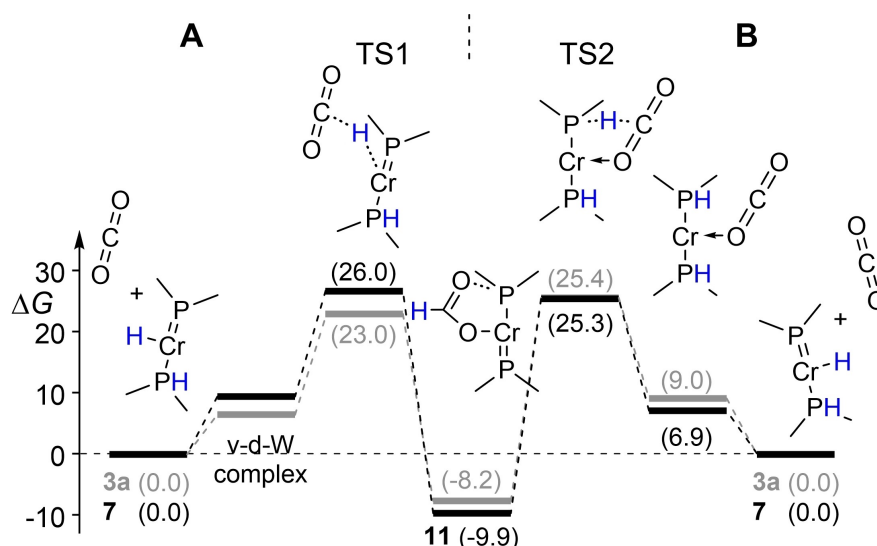


**Figure 5.** Schematic representation of the minimum energy reaction pathways (MERP) for the formation of formato complexes from **3a/7** and  $\text{CO}_2$  according to the 'outer sphere' (route A) and 'inner sphere' (route B) mechanism. Figures in parentheses denote computed (RI- $\omega$ B97x-D/def2-TZVP//RI- $\omega$ B97x-D/def2-SVP) standard Gibbs free energies ( $\Delta G^\circ$ ) in  $\text{kcal mol}^{-1}$  at stationary states on the MERP. Elements drawn in black (grey) refer to the reaction of **7** (**3a**). (v-d-W complex = van der Waals complex)

formate. The reaction proceeds under mild conditions using an iridium complex with a chelating abnormal NHC ligand as catalyst.<sup>[37]</sup>

To explore the feasibility of Cr-catalyzed transfer hydrogenation, we investigated the reaction of AB with  $\text{CO}_2$  (initial pressure 3.5 bar) in THF in the presence of **7** (0.5 mol-% relative to AB). NMR spectroscopy revealed the complete conversion of **7** into **11**, as well as the formation of over-stoichiometric quantities of cyclotriborazane<sup>[38]</sup> (CTB,  $(\text{H}_2\text{NBH}_2)_3$ ) and formylated ammonia boranes assigned as  $[\text{BH}_n(\text{OCHO})_{3-n}(\text{NH}_3)]$ , by analogy to the known<sup>[39]</sup> borates  $[\text{BH}_n(\text{OCHO})_{4-n}]^-$  ( $n = 1, 2$  in both cases). The observed generation of  $\text{H}_2$  implies that CTB arises at least in part from dehydrogenation of AB,<sup>[40]</sup> which obviously occurs as a side reaction. When the reaction proceeded, the initial products were further transformed into new species which contain according to their  $^{11}\text{B}$  NMR chemical shifts both three- and four-coordinate boron centers, and give rise to  $^1\text{H}$  NMR signals characteristic for methoxy groups. Based on their spectral data and the formation of methanol upon hydrolysis (vide infra), we formulate these products as methyl borates  $[\text{MeO}]_4\text{BX}_n^-$  and  $(\text{MeO})_n\text{BX}_{3-n}$  ( $n = 1-3$ , X = unspecified substituents), respectively. The NMR-based assignments were supported by MS studies, which allowed the detection of the mixed anhydride  $\text{B}(\text{OCHO})_3$  and traces of  $\text{B}(\text{OMe})_3$ , and the finding that work-up of a reaction mixture containing the assumed formyl borates furnished a solid, ether-insoluble material which hydrolyzed to give a weakly alkaline solution comprising  $\text{HCO}_2^-$ , boric acid,  $[\text{H}_2\text{B}(\text{OH})_2]^-$  and  $\text{NH}_3/\text{NH}_4^+$ , respectively.

To further optimize the  $\text{CO}_2$ -reduction and verify the catalytic activity of the chromium complexes, we studied the kinetics and product selectivity of transfer hydrogenations with different pre-catalysts (**5**, **7**, **11**). As a control, reactions using the degradation products **4H** and **8** resulting from thermal decay of

**7** as well as the uncatalyzed reaction of AB with  $\text{CO}_2$  were also investigated.

The reactions using **7** and **11** (Table 1, entries 1–3) proceeded with complete consumption of AB, whereas with **5** (entry 4) the conversion remained incomplete even after prolonged time and the experiment was terminated prematurely. All three reactions gave variable proportions of products featuring formyl and methoxy moieties, which were converted to methanol, formate, and formamide,<sup>[41]</sup> respectively, after addition of  $\text{H}_2\text{O}$  (Figure S19). Furthermore, CTB was in all cases detected as an intermediate. The overall turnover to  $\text{CO}_2$ -reduction products (determined from the total hydride equivalents transferred) followed, after an induction period in the reaction using **5**, in the early stages a pseudo-first-order rate law, which enabled us to compute average turnover frequencies (TOF) for comparing catalyst activities (Figure 6). In the control experiments (Table 1, entries 4–6), the consumption of AB and the amount of formyl species produced were far lower, and methoxylated products were not detectable at all.

The highest activity among all catalysts tested was observed for **11**. Raising the reaction temperature from 30 to 40 °C resulted in the expected speeding up of the overall reaction, but also in a significantly higher fraction of methylated species.<sup>[42]</sup> This trend implies that the reduction of formate is more accelerated than its formation from  $\text{CO}_2$ , which we attribute at least in part to the decreasing solubility of  $\text{CO}_2$  in the solution as the temperature rises. Formato complex **11** was for large parts of the reaction the only detectable phosphorus-containing species, indicating that it is probably the resting state of the catalyst. After longer reaction times, minor amounts of decomposition products (phosphine **4H** and its complex **8**) were also detectable.

The reaction using **7** (entry 3) proceeded at a reduced rate and gave lower conversion to formyl and methoxy derivatives

Entry	Precatalyst	T/°C	t/h	Conversion/% <sup>[b]</sup>			TON <sup>[f]</sup>	TOF <sup>[g]</sup> /h <sup>-1</sup>
				%(AB) <sup>[c]</sup>	%(OCHO) <sup>[d]</sup>	%(OCH <sub>3</sub> ) <sup>[e]</sup>		
1	<b>11</b> (0.4 mol-%)	30	140	> 99	14	17	2.4 · 10 <sup>2</sup>	5.1
2	<b>11</b> (0.4 mol-%)	40	63	> 99	8	25	2.6 · 10 <sup>2</sup>	8.9
3	<b>7</b> (0.4 mol-%)	30	280	> 99	10	15	2.0 · 10 <sup>2</sup>	0.74
4	<b>5</b> (0.4 mol-%)	30	285	86	13	15	2.2 · 10 <sup>2</sup>	1.0
5	<b>8</b> (0.4 mol-%)	40	150	14	5	0	34	n.d.
6	<b>4H</b> (1 mol-%)	40	160	10	3	0	9	n.d.
7	–	40	150	6.5	2	0	–	–

[a] Reaction conditions: 238–248 μmol NH<sub>3</sub>BH<sub>3</sub> und 0.95–2.2 μmol precatalyst in THF-D<sub>8</sub> (0.35 mL), 3.5 bar CO<sub>2</sub> [b] determined by integration of suitable <sup>1</sup>H NMR signals [c] fraction of AB consumed in % of the amount present at t=0: %(AB) = 100 · n(AB)<sub>t=t<sub>max</sub></sub>/n(AB)<sub>t=0</sub> [d] Yield of spectroscopically detectable formyl equivalents in %: %(OCHO) = 100/3 · n(OCHO)<sub>t=t<sub>max</sub></sub>/n(AB)<sub>t=0</sub> [e] Yield of spectroscopically detectable methoxy equivalents in %: %(OCH<sub>3</sub>) = 100 · n(OCH<sub>3</sub>)<sub>t=t<sub>max</sub></sub>/n(AB)<sub>t=0</sub> [f] number of CH-bonds formed per molecule of precatalyst: TON = (n(OCHO) + 3 · n(OCH<sub>3</sub>))/n(pre-cat)<sub>t=0</sub> [g] average turnover frequency TOF = ΔTON/Δt from regression analysis of the linear regime of the time-conversion curves displayed in Figure 6.

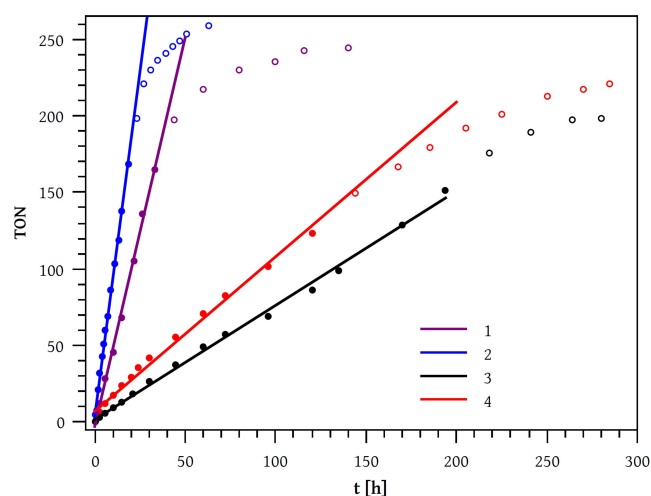


**Figure 6.** Time-conversion curves for the transfer hydrogenation of CO<sub>2</sub> with AB in the presence of bzNHP complexes. Data points refer to the entries 1–4 in Table 1. The straight lines represent the results of linear regression analyses performed on the linear regime of the curves.

at the cost of a higher production of H<sub>2</sub> from AB dehydrogenation. The extent of the side reaction seemed to drop off somewhat as the conversion of **7** to **11** increased. The reduced rate of the CO<sub>2</sub>-reduction compared to the previous reactions is most likely attributable to the decay of a significant fraction of the active complex to give catalytically less effective (vide infra) phosphine **4H** and its complex **8**, respectively.

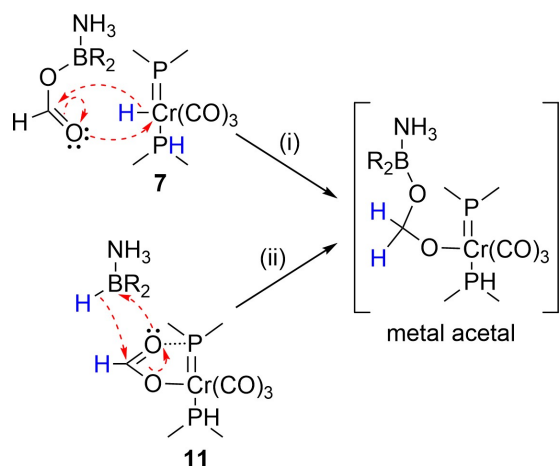
Compared to **7**, the use of bis-NHP complex **5** (entry 4) gave increased conversion to CO<sub>2</sub> reduction products at a slightly higher rate. Complexes **7** and **11** were not directly observable by NMR spectroscopy, but earlier findings by Gediga, who had noted that action of AB on bis-NHP complexes of tungsten gives rise to a heavier homologue of **7**,<sup>[43]</sup> suggest that the formation of **7** should likewise be feasible under the reaction conditions. This hypothesis is also in accord with the detection of phosphine **4H**, which had been identified as a thermal decomposition product of **7** (see supporting information). Starting from this conjecture, the CO<sub>2</sub> reduction could then

proceed according to the same mechanism as in the previous cases, with the lower activity compared to the reaction with **11** being attributable to a lower effective concentration of the active species.

The outcome of the control experiments implies that conversion of CO<sub>2</sub> to formate, but not its further reduction, also evolves without catalyst, and that this thermal background process is somewhat sped up by the presence of complex **8** or phosphine **4H** (which is converted into a borane adduct during the reaction). The modest catalytic activity of **8** arises possibly from its proven ability to lose CO (vide supra), which may give rise to trace amounts of **7** responsible for the catalysis. The insertion of CO<sub>2</sub> into BH-bonds being also aided by bases,<sup>[29–31]</sup> the still smaller accelerating effect of **4H** is probably attributable to its Lewis-base character which renders the observed phosphine borane more active than AB itself.

Summarizing the outcome of the kinetic studies, we conclude that the Cr-catalyzed CO<sub>2</sub>-reduction benefits from conditions suited to minimize the concentration of **7**, which is susceptible to decay causing catalyst deactivation, and concurrently maximize the concentration of **11**. While all bzNHP complexes are still less active than Choudhouri's Ir-complexes,<sup>[37]</sup> they offer nonetheless the advantage of carrying the reduction of CO<sub>2</sub> beyond the stage of formate—the transfer hydrogenation of CO<sub>2</sub> to methanol with NH<sub>3</sub>BH<sub>3</sub> is to the best of our knowledge yet undescribed for precious metal-based catalysts.

Although there is currently no experimental or computational evidence to support a mechanistic interpretation of the further reduction of formylated ammonia boranes or formate complex **11**, we envisage that these reactions could take a similar route as transition metal catalyzed CO<sub>2</sub> hydroboration.<sup>[44–47]</sup> The initial step would then involve action of AB on **11** or insertion of the formate unit of [BH<sub>n</sub>(OCHO)<sub>3–n</sub>(NH<sub>3</sub>)] into the Cr–H bond of **7** to produce a metal acetal (Scheme 6). Species of this type are considered transient intermediates in CO<sub>2</sub> hydroboration whose forthright reduction to methyl borates is well established.<sup>[47,48]</sup> The generation of a metal acetal



**Scheme 6.** Schematic representation of proposed reactions of (i) **7** with formylated ammonia boranes and (ii) **11** with AB to produce a transient metal acetal ( $R = \text{H}, \text{OCHO}$ ).

by reduction of a formate in the coordination sphere of a transition metal (Scheme 6, (ii)) adds a new facet that has been neglected in the mechanistic analyses of  $\text{CO}_2$  hydroboration,<sup>[47,48]</sup> but seems viable in view of the activating effect<sup>[47]</sup> arising from the secondary interaction of the formate ligand in **11** with the Lewis acidic NHP unit.

With the catalysis itself clearly proven, a remaining problem in all reactions is on the other hand the inefficient conversion of AB. This is probably due to the dehydrogenation with release of  $\text{H}_2$ , which seems in fact to be the main reaction. So far, a reaction temperature around  $40^\circ\text{C}$  proved beneficial for facilitating the further reduction of the formyl intermediates, but we note that still higher temperatures are expected to be unfavorable as they would further facilitate the thermally induced decomposition of AB.<sup>[40]</sup> Moreover, in view of the proven catalysis of AB dehydrogenation by a NHP complex of Mn,<sup>[49]</sup> we cannot exclude that the Cr complexes also accelerate the side reaction.

## Conclusions

Benzenellation increases the  $\pi$ -acceptor character of the P-based ligands in a bis-bzNHP complex of chromium. This leaves the complex not only more easily reducible than a congener carrying ligands with isolated heterocyclic rings, but also alters its chemical properties. Thus, while photo-reaction with  $\text{H}_2$  still gives rise to a  $\sigma\text{-H}_2$ -complex, the bzNHP ligands make this species a much less active catalyst in alkene hydrogenation and reduce also its thermal stability, which in turn compromises the selectivity of the isomerization under fission of the H–H bond and transfer of a hydride to one of the P-ligands. The phosphine-bzNHP-hydrido-complex resulting from this isomerization could be prepared by independent synthesis. It is more resilient towards loss of  $\text{H}_2$  than its non-anellated congener while exposing at the same time increased intramolecular mobility of P- and Cr-bound hydrogens. The combination of

fluxional structure and higher Lewis-acidity of the metal center facilitate the reversible attachment of an additional donor ligand at chromium as well as the reductive capture of  $\text{CO}_2$  to yield an isolable formato complex. Computational studies indicate that this reaction can proceed in principle via an 'inner sphere' pathway under direct transfer of the Cr-bound hydride to  $\text{CO}_2$ , or via a cooperative 'outer sphere' mechanism involving binding of  $\text{CO}_2$  by the metal and hydride transfer from a phosphine, which is in this case slightly favored due to steric reasons. The discovery that the original bzNHP-metal hydride is recyclable upon reaction of the formato complex with ammonia borane further paved the way for the proof-of-principle that bzNHP-complexes of chromium can catalyze the transfer hydrogenation of  $\text{CO}_2$  to methanol with ammonia borane, which is a reaction yet unknown for noble metal-based catalysts. Notwithstanding this achievement, further work is obviously needed to increase the overall catalytic activity and the selectivity for methoxylated products. Considering that Lewis-acidic cocatalysts promote the formation of methoxy boranes in the closely related metal catalyzed hydroboration of  $\text{CO}_2$ ,<sup>[47]</sup> the exploration of complexes with sterically less demanding but even more electron withdrawing bzNHP units appears to be a promising approach.

## Experimental Section

Manipulations were carried out under an atmosphere of inert argon inside glove boxes or by using standard vacuum line techniques unless stated otherwise. Solvents were dried by published procedures.<sup>[50]</sup> NMR spectra were recorded on Bruker Avance 250 ( $^1\text{H}$  250.0 MHz,  $^{31}\text{P}$  101.2 MHz) or Avance 400 ( $^1\text{H}$  400.1 MHz,  $^{13}\text{C}$  100.5 MHz,  $^{31}\text{P}$  161.9 MHz) instruments at 293 K.  $^1\text{H}$  Chemical shifts were referenced to TMS using the signals of the residual protons of the deuterated solvent ( $\text{C}_6\text{D}_6$ :  $\delta^1\text{H}$  7.15;  $\text{THF-d}_8$ :  $\delta^1\text{H}$  = 1.73) as secondary reference. Spectra of heteronuclei were referenced using the  $\Xi$ -scale<sup>[51]</sup> with TMS ( $\Xi$  = 25.145020 MHz,  $^{13}\text{C}$ ),  $\text{BF}_3 \cdot \text{OEt}_2$  ( $\Xi$  = 32.083974 MHz,  $^{11}\text{B}$ ) and 85%  $\text{H}_3\text{PO}_4$  ( $\Xi$  = 40.480747 MHz,  $^{31}\text{P}$ ) as secondary references. Reactions under elevated gas pressure were carried out in  $\text{C}_6\text{D}_6$  or  $\text{THF-d}_8$  using commercially available NMR tubes (Norell© Extreme Series) that could be flange-mounted to home-built apparatuses for the admission of  $\text{H}_2$ ,  $\text{CO}$ , and  $\text{CO}_2$ , respectively, under inert conditions. The gas pressure was adjusted at room temperature by controlling the total pressure in the apparatus determined by means of a manometer. Carbon monoxide (purity 3.7) and carbon dioxide were used as is, while hydrogen (purity 5.0) was purified using a SAES Pure Gas© (MC50-904 F) unit. Irradiation experiments were performed using an LSB523 150 W Xe OF xenon arc lamp in conjunction with an LSH102 air-cooled enclosure with LSC121 amplifying mirror purchased both from LOT Quantum Design. Further details on instruments and methods used for spectroscopic characterization and the procedures used for carrying out and evaluating the various reaction studies are included together with the appropriate data in the supporting information.

Deposition numbers 2282420 (4[ $\text{AlCl}_3 \cdot \text{Br}_0.5$ ]), 2282421 (**4H**), 2282422 (**5**), 2282423 (**8**), 2282424 (**10**), 2282425 (**9**), 2282426 (**4Br**), and 2282427 (**11**) contain the supplementary crystallographic data for this paper. These data are provided free of charge by the joint Cambridge Crystallographic Data Centre and Fachinformationszentrum Karlsruhe Access Structures service. Further crystallographic

data and details on the structure refinement are given in the Supporting Information.

RI-DFT calculations were carried out on the bwForCluster Justus2 with the TURBOMOLE program suite (version 7.5.2020).<sup>[52]</sup> Energy optimization of molecular structures and calculation of harmonic frequencies was carried out using the  $\omega$ B97x-D functional,<sup>[53]</sup> whose suitability for describing molecular structures of the NHP-complexes had already been shown,<sup>[3,4]</sup> with a def2-SVP basis set<sup>[54]</sup> on isolated molecules, simulating gas phase conditions. The stationary points located were identified as local minima on the energy hypersurface by harmonic vibrational frequency calculations at the same level. Electronic energies at the stationary points were recalculated with a def2-TZVP basis set<sup>[54]</sup> and are given at the RI- $\omega$ B97x-D/def2-TZVP//RI- $\omega$ B97x-D/def2-SVP level. Standard Gibbs free energies  $\Delta G^{298}$  were calculated using the def2-TZVP energies with the corrections obtained from the frequency calculations with the smaller basis set.

## Acknowledgements

The authors acknowledge support by the state of Baden-Württemberg through bwHPC and the German Research Foundation (DFG) through grant no INST 40/575-1 FUGG (JUSTUS 2 cluster) for the computational studies. We also thank C. Guttroff and Dr. W. Frey (Institute of Organic Chemistry) for the recording of mass spectra and the collection of XRD data sets, L. Dettmann and Dr. M. Ringenberg for measuring CVs and IR- and UV/VIS-SEC data, and Prof. Dr. B. Sarkar for granting generous access to (spectro)electrochemistry facilities. Open Access funding enabled and organized by Projekt DEAL.

## Conflict of Interests

The authors declare no conflict of interest.

## Data Availability Statement

The data that support the findings of this study are available in the supplementary material of this article.

**Keywords:** P ligands · N-heterocyclic phosphonium complexes · Benzanellation · Metal-ligand cooperative effects · CO<sub>2</sub>-reduction

- [1] a) T. P. Gonçalves, I. Dutta, K.-W. Huang, *Chem. Commun.* **2021**, 57, 3070; b) J. R. Khusnutdinova, D. Milstein, *Angew. Chem. Int. Ed.* **2015**, 54, 12236; c) W. I. Dzik, J. I. van der Vlugt, J. N. H. Reek, B. de Bruin, *Angew. Chem. Int. Ed.* **2011**, 50, 3356; d) H. Grützmacher, *Angew. Chem. Int. Ed.* **2008**, 47, 1814.
- [2] a) L. Alig, M. Fritz, S. Schneider, *Chem. Rev.* **2019**, 119, 2681; b) F. Kallmeier, R. Kempe, *Angew. Chem. Int. Ed.* **2018**, 57, 46; c) G. A. Filonenko, R. van Putten, E. J. M. Hensen, E. A. Pidko, *Chem. Soc. Rev.* **2018**, 47, 1459; d) N. A. Eberhardt, H. Guan, *Chem. Rev.* **2016**, 116, 8373; e) S. Chakraborty, P. Bhattacharya, H. Dai, H. Guan, *Acc. Chem. Res.* **2015**, 48, 1995.
- [3] N. Birchall, C. M. Feil, M. Gediga, M. Nieger, D. Gudat, *Chem. Sci.* **2020**, 11, 9571.

- [4] N. Birchall, M. Nieger, D. Gudat, *ChemPlusChem* **2024**, e202400144; <https://doi.org/10.1002/cplu.202400144>.
- [5] N. Burford, A. I. Dipchand, B. W. Royan, P. S. White, *Acta Cryst. C* **1989**, 45, 1485.
- [6] D. Schmid, D. Bubrin, D. Förster, M. Nieger, E. Roeben, S. Strobel, D. Gudat, *C. R. Chim.* **2010**, 13, 998.
- [7] B. Rao, C. C. Chong, R. Kinjo, *J. Am. Chem. Soc.* **2018**, 140, 652.
- [8] D. M. C. Ould, A. C. Rigby, L. C. Wilkins, S. J. Adams, J. A. Platts, S. J. A. Pope, E. Richards, R. L. Melen, *Organometallics* **2018**, 37, 712.
- [9] N. Burford, A. I. Dipchand, B. W. Royan, P. S. White, *Inorg. Chem.* **1990**, 29, 4938.
- [10] D. Schmid, S. Loscher, D. Gudat, D. Bubrin, I. Hartenbach, T. Schleid, Z. Benkó, L. Nyulászi, *Chem. Commun.* **2009**, 830.
- [11] M. Gediga, S. H. Schlindwein, J. Bender, M. Nieger, D. Gudat, *Angew. Chem. Int. Ed.* **2017**, 56, 15718.
- [12] T. Janes, J. M. Rawson, D. Song, *Dalton Trans.* **2013**, 42, 10640.
- [13] S. Burck, D. Gudat, M. Nieger, Z. Benko, L. Nyulaszi, D. Szieberth, *Z. Anorg. Allg. Chem.* **2009**, 635, 245.
- [14] C. A. Caputo, A. L. Brazeau, Z. Hynes, J. T. Price, H. M. Tuononen, N. D. Jones, *Organometallics* **2009**, 28, 5261.
- [15] D. Herrmannsdörfer, M. Kaaz, O. Puntigam, J. Bender, M. Nieger, D. Gudat, *Eur. J. Inorg. Chem.* **2015**, 4819.
- [16] G. A. Abakumov, N. O. Druzhkov, G. G. Kazakov, G. K. Fukin, R. V. Rummyantsev, V. K. Cherkasov, *Dokl. Chem.* **2019**, 489, 279.
- [17] C. A. Caputo, M. C. Jennings, H. M. Tuononen, N. D. Jones, *Organometallics* **2009**, 28, 990.
- [18] A. W. Addison, T. N. Rao, J. Reedijk, J. van Rijn, G. C. Verschoor, *J. Chem. Soc. Dalton Trans.* **1984**, 1349.
- [19] D. G. Hamilton, R. H. Crabtree, *J. Am. Chem. Soc.* **1988**, 110, 4126.
- [20] G. J. Kubas, *Acc. Chem. Res.* **1988**, 21, 120.
- [21] R. H. Crabtree, *Acc. Chem. Res.* **1990**, 23, 95.
- [22] P. J. Desrosiers, L. Cai, Z. Lin, R. Richards, J. Halpern, *J. Am. Chem. Soc.* **1991**, 113, 4173.
- [23] Regardless of the presence of identical N-substituents in **2a** and **6**, the anellation reduces the conformational flexibility of the NHP unit, which may obstruct the necessary conformational changes during a reaction.
- [24] However, we want to note that the observation of visible line broadenings for the <sup>1</sup>H and <sup>31</sup>P{<sup>1</sup>H} NMR signals of the nuclei in the PH-moieties of **10** is compatible with the complex being in dynamic equilibrium with undetectable trace amounts of dissociation products.
- [25] C. C. Chong, R. Kinjo, *Angew. Chem. Int. Ed.* **2015**, 54, 12116.
- [26] C. C. Chong, R. Kinjo, *ACS Catal.* **2015**, 5, 3238.
- [27] D. J. Darensbourg, A. Rokicki, *Organometallics* **1982**, 1, 1685.
- [28] D. J. Darensbourg, H. P. Wiegrefe, P. W. Wiegrefe, *J. Am. Chem. Soc.* **1990**, 112, 9252.
- [29] T.-X. Zhao, G.-W. Zhai, J. Liang, P. Li, X.-B. Hu, Y.-T. Wu, *Chem. Commun.* **2017**, 53, 8046.
- [30] T. Zhao, C. Li, X. Hu, F. Liu, Y. Wu, *Int. J. Hydrogen Energy* **2021**, 46, 15716.
- [31] B. Zhang, G. Du, W. Hang, S. Wang, C. Xi, *Eur. J. Org. Chem.* **2018**, 1739.
- [32] G. Ménard, D. W. Stephan, *J. Am. Chem. Soc.* **2010**, 132, 1796.
- [33] G. Ménard, D. W. Stephan, *Dalton Trans.* **2013**, 42, 5447.
- [34] A. Jana, D. Ghoshal, H. W. Roesky, I. Objartel, G. Schwab, D. Stalke, *J. Am. Chem. Soc.* **2009**, 131, 1288.
- [35] A. Jana, G. Tavcar, H. W. Roesky, M. John, *Dalton Trans.* **2010**, 39, 9487.
- [36] A. Jana, H. Roesky, C. Schulzke, A. Döring, *Angew. Chem. Int. Ed.* **2009**, 48, 1106.
- [37] A. Kumar, J. Eyyathiyil, J. Choudhury, *Inorg. Chem.* **2021**, 60, 11684.
- [38] J. S. Wang, R. A. Geanangel, *Inorg. Chim. Acta* **1988**, 148, 185.
- [39] I. Knopf, C. C. Cummins, *Organometallics* **2015**, 34, 1601.
- [40] A. Staubitz, A. P. M. Robertson, I. Manners, *Chem. Rev.* **2010**, 110, 4079.
- [41] L. Hao, H. Zhang, X. Luo, C. Wu, Y. Zhao, X. Liu, X. Gao, Y. Chen, Z. Liu, *J. CO<sub>2</sub> Util.* **2017**, 22, 208.
- [42] The presence of residual formyl species at the end of the reactions is attributable to the fact that the amount of AB used was insufficient for complete conversion.
- [43] M. Gediga, *Dissertation*, University of Stuttgart, **2017**, DOI: <https://doi.org/10.18419/opus-9410>.
- [44] S. Chakraborty, J. Zhang, J. A. Krause, H. Guan, *J. Am. Chem. Soc.* **2010**, 132, 8872.
- [45] R. Pal, T. L. Groy, R. J. Trovitch, *Inorg. Chem.* **2015**, 54, 7506.
- [46] L. J. Murphy, H. Hollenhorst, R. McDonald, M. Ferguson, M. D. Lumsden, L. Turculet, *Organometallics* **2017**, 36, 3709.
- [47] M. R. Espinosa, D. J. Charboneau, A. Garcia de Oliveira, N. Hazari, *ACS Catal.* **2019**, 9, 301.

- [48] F. Huang, C. Zhang, J. Jiang, Z.-X. Wang, H. Guan, *Inorg. Chem.* **2011**, *50*, 3816.
- [49] M. Gediga, C. M. Feil, S. H. Schlindwein, J. Bender, M. Nieger, D. Gudat, *Chem. Eur. J.* **2017**, *23*, 11560.
- [50] W. L. F. Armarego, C. L. L. Chai, *Purification of Laboratory Chemicals*, 5th ed, Butterworth-Heinemann, Amsterdam, **2003**.
- [51] R. H. Harris, E. D. Becher, S. M. C. de Menezes, R. Goodfellow, P. Granger, *Concepts Magn. Reson.* **2002**, *14*, 326.
- [52] a) TURBOMOLE V7.5 2020, a development of University of Karlsruhe and Forschungszentrum Karlsruhe GmbH, 1989–2007, TURBOMOLE GmbH, since 2007; available from <https://www.turbomole.org>; b) S. G. Balasubramani, G. P. Chen, S. Coriani, M. Diedenhofen, M. S. Frank, Y. J. Franzke, F. Furche, R. Grotjahn, M. E. Harding, C. Hättig, A. Hellweg, Helmich-Paris, C. Holzer, U. Huniar, M. Kaupp, A. Marefat Khah, S. Karbalaeei Khani, T. Müller, F. Mack, B. D. Nguyen, S. M. Parker, E. Perlt, D. Rappoport, K. Reiter, S. Roy, M. Rückert, G. Schmitz, M. Sierka, E. Tapavicza, D. P. Tew, C. van Wüllen, V. K. Voora, F. Weigend, A. Wodyński, J. M. Yu, *J. Chem. Phys.* **2020**, *152*, 184107B.
- [53] J.-D. Chai, M. Head-Gordon, *Phys. Chem. Chem. Phys.* **2008**, *10*, 6615.
- [54] F. Weigend, R. Ahlrichs, *Phys. Chem. Chem. Phys.* **2005**, *7*, 3297.

---

Manuscript received: April 30, 2024

Accepted manuscript online: June 11, 2024

Version of record online: July 30, 2024